Case Studies in Construction Materials 22 (2025) e04810

Contents lists available at ScienceDirect

Case Studies in Construction Materials

journal homepage: www.elsevier.com/locate/cscm

Short communication

Experimental and numerical investigation on clogging by trapped solid particles in permeable porous concrete

Carlos Ignacio Vizcaíno-López [a,1], Martín Hernández-Marín [b,*,2], Gil Humberto Ochoa-González [c,3], Lilia Guerrero-Martínez [d,4], Isaí Gerardo Reyes-Cedeño [e,5], Anuard Isaac Pacheco-Guerrero [f,6]

[a] Doctorado en Ciencias de los Ámbitos Antrópicos, Autonomous University of Aguascalientes, Mexico
[b] Department of Civil Engineering, Autonomous University of Aguascalientes, Mexico
[c] Department of Habitat and Urban Development, ITESO Jesuit University of Guadalajara, Mexico
[d] Department of Civil Engineering, Autonomous University of Aguascalientes, Mexico
[e] Universidad Panamericana, Facultad de Ingeniería, Jose María Escrivá de Balaguer 101, Villas Bonaterra, Aguascalientes, 20296, México
[f] Engineering Academic Unit I, Autonomous University of Zacatecas, Mexico

ARTICLE INFO

Keywords:
Permeable porous concrete
Pore clogging
Numerical simulation model
Permeability
Seepage velocity

ABSTRACT

Clogging due to entrapment of solid particles in pores is a recurring process that limits the performance of permeable porous concrete (PPC). In this work, an analysis based on the results of laboratory and numerical modelling is presented. The experimental work involved the preparation and testing of PPC cylindric samples (100 mm diameter and 160 mm in height) to obtain the porosity and permeability parameters, and based on these two, the seepage velocity. These three parameters were used as inputs in the further numerical models, which were accomplished with the commercial software COMSOL Multiphysics v.6.2, based on the finite element method. Two scenarios with six simulations (3 each) were performed using three types of materials as solid particles, as well as two dimensional samples with the dimensions of the experimental samples. From the experimental work we found that the porosity and permeability varied from 26 % to 28 % and 1.75–1.96 mm/s, respectively, and from these parameters the calculated seepage velocity varied from 8.28 to 9.61 mm/s. However, for a comparative analysis, a different value of seepage velocity was used in each modelling scenario: the resulting from the experimental work, this is 8.98 mm/s for scenario 1, while for scenario 2, a value of 2.43 mm/s was used, which corresponds to the minimum recommended for the performance of PPC, according to American Concrete Institute ACI 522 R technical report. In the numerical work, we observed that the reduced seepage velocity of scenario 2 permitted the exit of particles from the model in all cases.

* Corresponding author.
E-mail addresses: vizlopcar@hotmail.com (C.I. Vizcaíno-López), martin.hernandez@edu.uaa.mx (M. Hernández-Marín), gilochoa@iteso.mx (G.H. Ochoa-González), lilia.guerrero@edu.uaa.mx (L. Guerrero-Martínez), igreyes@up.edu.mx (I.G. Reyes-Cedeño), anuard.pacheco@uaz.edu.mx (A.I. Pacheco-Guerrero).
[1] 0000-0002-3001-0176
[2] 0000-0002-9420-0403
[3] 0000-0002-3699-0443
[4] 0000-0002-7769-1335
[5] 0009-0002-4681-1311
[6] 0000-0003-4876-7115

https://doi.org/10.1016/j.cscm.2025.e04810
Received 18 February 2025; Received in revised form 12 April 2025; Accepted 20 May 2025
Available online 21 May 2025

1. Introduction

The demand of sustainable building materials has increased in recent years due to modern environmental challenges [1–3]. One of these materials commonly used in urban areas is permeable porous concrete (PPC), which is designed to allow free infiltration of water into the soil, where the negative effects of flooding and high temperatures need to be mitigated [3–5]. Although the zones in urban areas available for the application of PPC are limited, some others such as parking lots, industrial parks, and secondary roads have the potential for its implementation [6]. However, one of the most recurrent processes affecting PPC performance is clogging by solids, which typically results in a progressive reduction in permeability [7–10]. Clogging in PPC is a complex process because the porous network of PPC is highly heterogeneous, with variable pore diameters, multiple branching of pore tubes, and tortuous flow paths [10–12]. Under operating conditions, the solid inorganic particles that induce clogging in PPC include sediments such as sand, silt, and clay from surrounding areas, which arrive by dragging due to runoff [13–15]. To understand the hydraulic performance of PPC, the results of experimental and numerical studies are presented and analysed, performing and studying characteristics such as 1) their intrinsic permeability obtained from laboratory tests; 2) the pore size measured from physical tests, and 3) the capacity of this material to permit the flux of solid particles in its porous net.

Physical and hydraulic properties such as porosity, surface area, tortuosity, pore size and permeability are commonly used to characterize transport phenomena in porous media. The values of some of these parameters is helpful in defining the type of porous media [16]. In the case of PPC, permeability presents typical values ranging from 2 to 5.3 mm/s, infiltration rate from 120 to 320 L/m^2/min, and porosity in the range of 15–25 % [17]. However, values outside these ranges have also been reported, for example, Sandoval et al. [10] obtained porosity and permeability values of 26.57 % and 10.27 mm/s, respectively, for PPC samples of 100 mm in diameter and 200 mm in height and using a constant head permeameter. Permeability values of 2 mm/s and low porosity of 14 % were also reported by Cai et al. [12]. They used an industrial instrument that measures permeability based on Darcy's law. These examples indicate that PPC can exhibit variability in most physical and hydraulic properties, regardless of the method used to obtain them.

The clogging of PPC by solids such as sediments and its effect on permeability reduction has been the subject of several experimental studies. For example, Coughlin et al. [18] constructed a laboratory-scale pavement system to measure clogging that consisted of a permeable concrete layer, a base layer, and a subgrade layer. They conclude that sodium-rich montmorillonite-type clay causes ten times more clogging than sand. Later, Sandoval et al. [10] found that clays from the city of Londrina, Paraná, composed in 50 % by particles of 0.001–0.075 mm, 50 % by particles smaller than 0.001 mm and a specific gravity of 3.03, had a greater influence on the clogging of the PPC than sands with sizes from 0.075 to 4.75 mm, due to plasticity effect that caused the formation of lumps inside the pores, achieving permeability reductions greater than 95 %. In another study by Hu et al. [19], four clogging granular materials (I through IV) were used and placed on a PPC pavement system that included a 100 mm top layer of 20 % porous PPC. Clogging materials I and II consisted of well-graded sands containing 90–95 % of particles from 0.075 to 2.36 mm and 5–10 % of particles smaller than 0.075 mm; clogging material III was poorly graded coarse sand containing only particles from 0.6 to 2.36 mm; and material IV was a poorly graded fine sand containing 93 % of particles from 0.075 to 0.6 mm and 7 % of particles smaller than 0.075 mm. The authors observed that well-graded materials caused severe clogging compared to poorly graded materials. Cai et al. [12] also proposed a novel method to evaluate PPC clogging using topsoil collected in Kaifeng, China as a saturated soil clogging suspension. Experimental research to evaluate PPC properties, such as those discussed here, can serve as a starting point, for example, as input data for the development of further investigations, such as those achieved in numerical studies.

Numerical studies related to PPC clogging include a wide range of computational tools such as specialized software, modules, algorithms and others. In this regard, Zhang et al. [20] developed a CFD-DEM model using the computational fluid dynamics (CFD) software Ansys Fluent coupled with commercial EDEM software, which uses the discrete element method (DEM) approach to simulate granular solids. The CFD-DEM numerical approach can predict particle trajectories by calculating the resultant force acting on each particle, including the drag force caused by the surrounding fluid flow [21]. In another study, Turco et al. [22] analysed the hydraulic behaviour of water flow through a PPC system, using HYDRUS-2D modelling and then validated it using an independent set of experimental data obtained from a laboratory-scale permeable pavement system. Nan et al. [23] investigated clogging of sand particles by performing experiments and further simulations in a CFD-DEM model. Computational tools such as software and modelling can be useful to understand and predict processes such as clogging in PPC using different physical scenarios.

Although several studies have evaluated the effect of clogging in PPC using numerical modelling, few use real parameters as inputs to their simulations. Therefore, the objective of this study is to provide knowledge on the process of clogging affecting the performance of PPC, by analysing the results of numerical models on PPC samples. The designed 2-dimensional numerical models contain a synthetic porous network with dimensions based on real cylindrical samples, while the parameters used in the simulations, particularly permeability and porosity, are based on the experimental results performed in this investigation. The commercial software COMSOL Multiphysics was used to perform the simulations and analyse the results. The questions we address in this investigation are: how long does it take for the PPC to become clogged by a flow of solid particles? How do heterogeneities in the pore network of the PPC influence the clogging by solid particles? And what is the main trajectory and velocity of solid particles that can cause clogging in PPC?

2. Methodology

The methodology to achieve the objectives of this investigation is based on two parts, experimental and numerical. From the experimental part the key parameters porosity and permeability were determined using cylindrical PPC samples, composed of Portland cement and river sand. In addition, a constant head permeameter was adapted to determine the permeability, while the porosity of the

samples was determined using the mass difference method. For the numerical part we used the commercial software COMSOL Multiphysics v. 6.2, which is based on the finite element method [24]. The finite element COMSOL Multiphysics was selected for the numerical analysis in this investigation because of its capability to: i) simulate the flow of particulate solids in closed channels, as observed in porous materials; ii) combine two or more physics in a single model; iii) allow temporal and spatial analysis of complex simulations; among other technical features. The simulations combined two modules of this software, the particle tracking module and the laminar flow module, using two-dimensional models based on the geometry of the laboratory samples. The parameters obtained in the experimental part were used as inputs in the numerical part.

2.1. Experimental work: preparation of samples and tests development

The parameters permeability and porosity were the main goal of the experimental work and are closely related to simulations, since they were used in the numerical section to obtain more realistic results of hydraulic obstruction occurring in PPC. For this purpose, PPC specimens were prepared using the basic materials Portland cement and aggregates of sand and gravel with subangular shapes. These aggregates were prepared using the Unified Soil Classification System (USCS), which resulted in a mixture of well-graded gravel and sand with uniformity and curvature coefficients of 4.36 and 1.98, respectively, as shown in Fig. 1. Regarding the mix proportioning of the PPC, the weight ratios of aggregate-cement and water-cement used in the mixture resulted in 4:1 and 0.33, respectively. In other words, 4 parts of aggregate were used for each part of cement, and 0.33 parts of water were used for each part of cement. In general, PPC samples were prepared for testing in accordance with ACI 522 R [25] and ASTM C192 [26] specifications.

In this case, a single PPC mix was used for all experiments. The mixture was designed to achieve a proper balance between porosity and permeability in the experiments, since as porosity increases, permeability increases but compressive strength decreases. Other mix designs were discarded because permeability was zero at porosities equal to or less than 15 %.

Basic parameters in the materials used in the samples, such as moisture content and density of the aggregates, were evaluated prior to testing. The moisture content of a representative sample of aggregates was determined and adjusted a few minutes before the PPC sample was prepared, while the density and absorption percentage of the aggregates used in sampling resulted of 2395 kg/m^3 and 3.77 %, respectively, according to the procedure of ASTM C127 [27]. After curing, which is a regular process to ensure that each type of concrete reaches its maximum properties of hardness and durability, the samples were cut to obtain the desired dimensions. In total, a set of 8 cylindrical specimens, 100 mm in diameter and 160 mm in height, were used in the tests, as shown in Fig. 2.

To obtain the porosity of the PPC samples, we applied the mass difference method, following to the ASTM C140 [28] standard. The formula is given by:

$$n = \left[1 - \frac{m_2 - m_1}{\rho_w V}\right] * 100 \tag{1}$$

Where n is the percentage of porosity, m_1 is the mass of the sample immersed in water (gr), m_2 is the mass of the dry sample (gr), V is the apparent volume of the sample (cm^3), and r_w is the density of water (gr/cm^3).

To obtain the vertical permeability of the PPC, a constant head permeameter was adapted to the dimensions of the samples. Part of this adaptation included ensuring free vertical water flow during the tests, which was achieved by laterally confining the PPC samples with 75 mm Humboldt latex membranes. The water flowing out of the samples was collected in a container underneath the sample so that the volume of water flowing out could be measured for further calculations. Fig. 3 shows the test procedure and a schematic of the permeameter used.

Permeability from the tests was finally estimated using Eq. 2, which is based on Darcy's law [29].

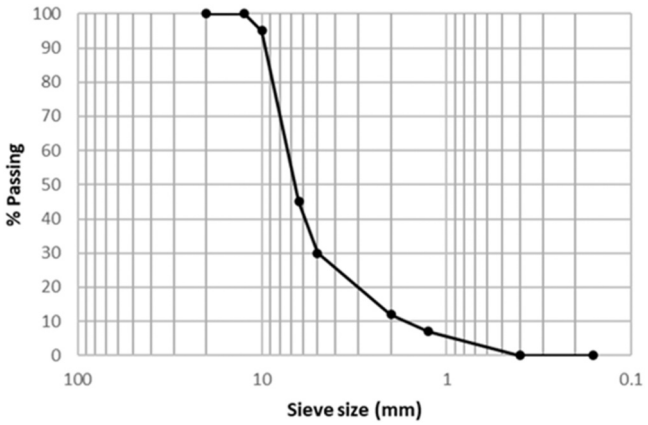

Fig. 1. Granulometric curve of the mixture of aggregates used in the preparation of PPC samples.

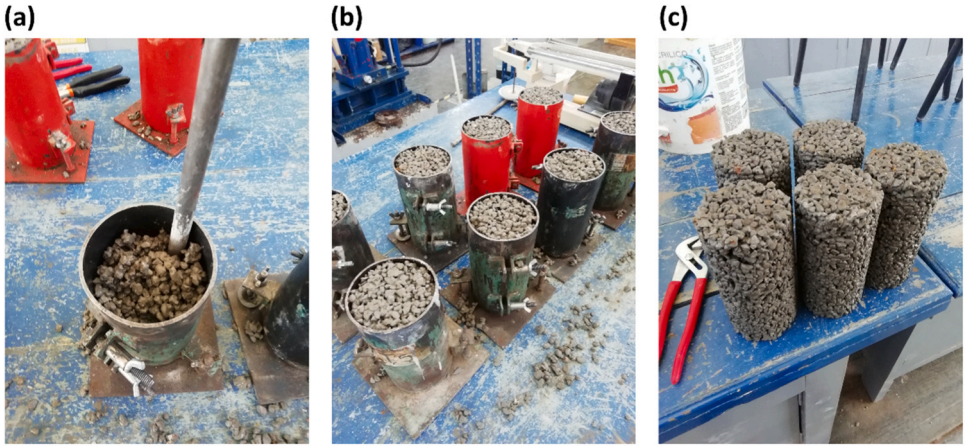

Fig. 2. Laboratory procedures for obtaining PPC samples. Incise (a) shows a stage of specimen preparation, (b) shows the set of specimens in molds for testing, and (c) shows some of the final specimens before testing.

$$k = \frac{Q \quad L}{A \quad H \quad t} \tag{2}$$

Where Q is the flow rate, t is the time in seconds that the volume of water needs to pass through the cross-sectional area A of the PPC sample. L is the length of the sample and H is the hydraulic head differential. As part of the calculations, a constant water height of 50 mm above the free surface of the PPC samples was used, since small values of constant head are applicable for Darcy's law and represent realistic conditions of water infiltration into the PPC during a storm [30].

2.2. Numerical modelling setup

Numerical simulations in COMSOL were applied to the PPC samples to represent and analyse real scenarios of clogging in different conditions of water-solid infiltration. For this purpose, the COMSOL software includes two modules, Particle Tracking and Laminar Flow, which permit to simulate the movement trajectories and the interaction of solid particles through porous materials such as PPC. For this work, the trajectories of particles such as sands moving through PPC were simulated based on the physical laws that influence the motion of solids. For instance, laminar flow for incompressible single-phase fluid, drag force, and gravity, among others, however, frictional forces have been omitted from the simulations because solid particles entering the PPC are simulated to be dragged by a water flow, which may instead reduce friction.

As part of the methodology, we used a two-dimensional model whose dimensions were based in the real samples used in the experimental part, this is 100 mm wide and 160 mm high, with the porosity numerically based on the porosity of the experimental part, is shown in Fig. 4a. The pore diameters varied from 2 to 8 mm and consisted in a synthetic nonlinear pore network with a geometry obtained from Image J v.1.54 dm, a software for digital image processing that allows to establish the desired porosity.

Two main boundary conditions were included in the construction of the model: restricted lateral flow representing the effect of the elastic membrane, and flow on the top and bottom of the model, simulating the inlet and outlet of water and particles into the PPC samples, as shown in Fig. 4a. For the correct performance of the numerical model, the inputs used in the simulations other than porosity and permeability, were relative inlet pressure, temperature, seepage velocity of water, particle diameter and particle release time. The outputs of the simulations for the further analysis involved the position, velocity and trajectory of the particles. Another relevant feature in the simulations is the insertion of the predefined coarse mesh depicted in Fig. 4b, which permitted to reduce the time of the simulations. In addition, a relative pressure of 490 Pa was simulated at the top of the model, simulating the 50 mm of water heigh used above the samples during the experiments. This relative pressure was set to increase linearly with depth during simulations reaching a value of 2060 Pa at the bottom of the model, as shown in Fig. 4c.

The selection of clogging materials was key in the simulations as this process depends mainly on the solids trapped in pores. For this, the particle tracking module for fluid flow in the software COMSOL provides some options for defining the size and number of solid particles, as well as the way in which the particles enter the model domain [24]. Based on this, the clogging solids used in simulations were equivalent in size to sand particles, since sand is a clogging material frequently found at PPC application sites, for example, during storm events when sediment and other similarly sized solid particles are carried along. [19]. Approximately 20 g of clogging particles were used in each simulation, separated into three types of materials, as specified in Table 1. Solid particles with diameters lower than that of material III were not considered in simulations due to the excessive time needed to complete them. For the analysis of the results in this part of the investigation, simulations were grouped and organized according to the available resources of computing and the expected results. Solid particles with diameters smaller than that of material III were not considered in the simulations due to the excessive time required. For the analysis of the results in this part of the investigation, the simulations were grouped and organized according to the available computational resources and the expected results.

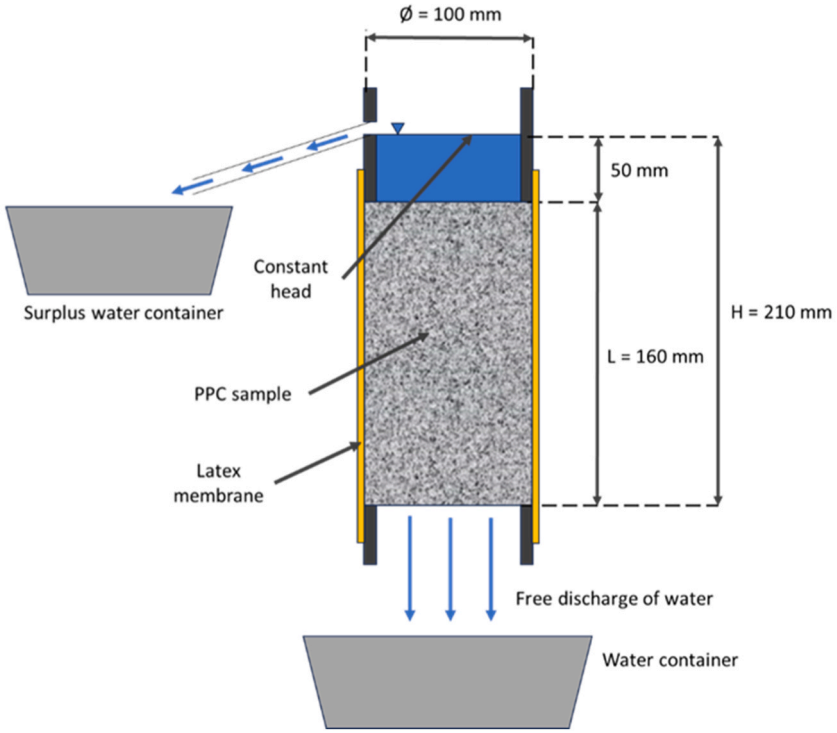

Fig. 3. Permeability test method for PPC samples and constant head permeameter scheme.

A total of 6 simulations were performed considering 2 different scenarios, depending on the seepage velocity parameter (v_s), which was determined by measuring the volume of water that passed through the cross section of each sample in approximately 20 seconds. Eq. 3 permit the estimation of seepage velocity [29].

$$v_s = \frac{Q}{A \quad t \quad n} \tag{3}$$

A value of 8.98 mm/s for vs was obtained with data from the experimental part and used in the first scenario. However, in the second scenario, a value of 2.43 mm/s was used, corresponding to a permeability of 0.5 mm/s. This value for permeability is the minimum recommended to ensure the hydraulic performance of a PPC pavement according to ACI 522 R [25] and was established in response to the real permanent reduction in effective porosity and permeability that PPC experience due to the unrestored pores after maintenance [10]. The numerical information in Table 2 shows the modelling parameters used for the different scenarios and simulations.

For better results in the numerical analysis, each of the two scenarios presents 6 simulations, and each of them is divided into 4 steps: step 1 corresponds to the time needed to release all the particles into the sample; step 2 indicates the time when the particles reach the sample outlet in at least 1 of the pores; step 3 indicates the time when the particles reach the sample outlet in all the pores (3

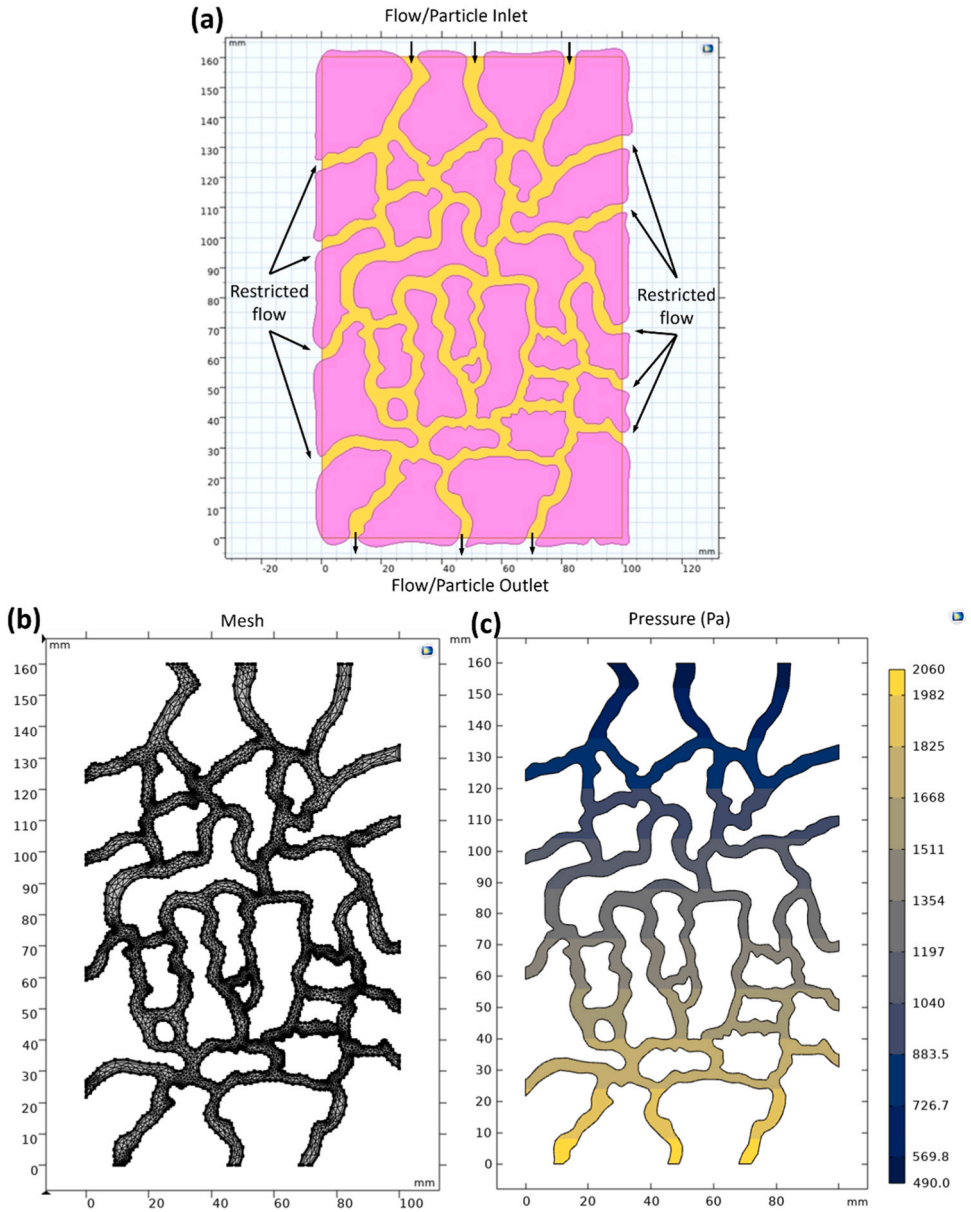

Fig. 4. Model domain and some of the main features used in the simulations. a) Conceptual model with the porous structure including boundary conditions, b) Meshing used in porous network, and c) relative pressure variation in pore fluids.

pores in total); finally, step 4 corresponds to the total time of the simulation, observed as the time when all the particles stopped moving in the simulation.

To ensure correct performance of the simulations, the particle release time was divided into 2 equal periods, each of which released 20 particles. Thus, for scenario 1 the particle release time for each period was 10 seconds, while for scenario 2 this time increased to 30 seconds. Each simulation was considered as complete when no movement of solid particles was observed, or when no exit of them from the simulated sample was recorded. To estimate the percentage of solid particles trapped within the PPC sample in each simulation, COMSOL permitted to place a virtual particle counter at the bottom of the model.

3. Results and discussion

3.1. Experimental results

The key parameter porosity obtained from the 8 samples presented a narrow range of variation, with a minimum of 26 %, resulted in one sample, a maximum of 28 % presented in two samples, and average of 27 % which also resulted in four samples and which, was

Table 1
Characteristics of granular clogging materials in the numerical simulations. To estimate the number and mass of solid particles, we considered a completely spherical shape and a density of 2650 kg/m^3, as reported by Das and Sobhan [29] for solid quartz sand particles.

Clogging Material	Diameter (size) (mm)	Number of particles	Total Particle mass (g)	Total Particle mass (%)
Material I 2.36–1.18 mm Very coarse sand	2.36	156	2.8451	14.2
	2.16	156	2.1814	10.9
	2	312	3.4633	17.3
	1.8	468	3.7871	18.9
	1.6	468	2.6598	13.3
	1.4	780	2.9698	14.8
	1.25	780	2.1138	10.6
Total		3120	20.0203	100.0
Material II 1.18–0.6 mm Coarse sand	1.18	1248	2.8451	13.9
	1.12	1248	2.4328	11.9
	1	2496	3.4633	16.9
	0.9	3744	3.7871	18.5
	0.8	3744	2.6598	13.0
	0.71	6240	3.0989	15.2
	0.63	6240	2.1650	10.6
Total		24960	20.4520	100.0
Material III 0.6–0.3 mm Medium sand	0.6	9984	2.9923	14.5
	0.56	9984	2.4328	11.8
	0.5	19968	3.4633	16.8
	0.45	29952	3.7871	18.4
	0.4	29952	2.6598	12.9
	0.355	49920	3.0989	15.0
	0.315	49920	2.1650	10.5
Total		199680	20.5992	100.0

Table 2
Modelling parameters used in simulations. The particle release time corresponds to the period in which the clogging materials enter the model from the top of the model. Two seconds after the release of particles, first allowing the laminar flow of water within the pores to stabilize.

Scenario	Simulation	Seepage velocity (mm/s)	Number of particles released	Particle releasing time (s)	Clogging material
1	1	8.98	3120	2–12	Material I
	2	8.98	24960	2–12	Material II
	3	8.98	199680	2–12	Material III
2	4	2.43	3120	2–32	Material I
	5	2.43	24960	2–32	Material II
	6	2.43	199680	2–32	Material III

finally used as input in the numerical part. Table 3 shows the experimental parameters used to obtain porosity using the mass difference method. The porosity results indicate that the sample preparation procedure was sufficiently homogeneous.

The parameters permeability and the seepage velocity presented also a narrow range of variation as can be observed in Table 4. Permeability varied from 1.75 to 1.96 mm/s, with an average value of 1.86 mm/s, while the seepage velocity varied from 8.28 to 9.61 mm/s, with an average value of 8.98 mm/s. As mentioned previously, the average value of seepage velocity was used in the first scenario of the simulations, while value of 2.43 mm/s was used in simulations for the second scenario.

3.2. Numerical results

Numerical results demonstrated a heterogeneous response of PPC samples under the flux of particles, depending on the simulated

Table 3
Porosity obtained from the experimental results.

Sample	Dry sample mass (gr)	Water-immersed sample mass (gr)	Sample apparent volume (cm^3)	Porosity (%)
1	2121	1191	1257	26
2	2109	1205	1257	28
3	2140	1220	1257	27
4	2133	1217	1257	27
5	2134	1228	1257	28
6	2130	1213	1257	27
7	2132	1218	1257	27
8	2115	1206	1257	28
Average				27

Table 4
Experimental results of permeability and seepage velocity.

Sample	Section (cm^2)	Water Volume (cm^3)*	Time (s)**	Porosity	Permeability (mm/s)	Seepage velocity (mm/s)
1	78.54	2290	119.46	0.26	1.86	9.38
2	78.54	2240	120.11	0.28	1.81	8.46
3	78.54	2440	120.53	0.27	1.96	9.61
4	78.54	2390	119.23	0.27	1.94	9.41
5	78.54	2190	120.62	0.28	1.76	8.28
6	78.54	2430	120.05	0.27	1.96	9.53
7	78.54	2280	119.72	0.27	1.85	8.89
8	78.54	2150	119.46	0.28	1.75	8.28
Average					1.86	8.98

* Water volume recovered in the container below the sample.
** Time needed for the water to drop out the sample.

conditions. Figs. 5 and 6 show the results of the completed simulations for scenarios 1 and 2, respectively, indicating the position, trajectory, and velocity of the particles.

From simulation 1, shown in Fig. 5, a predominance of blue tones can be observed in the pores of the models, thus the more prevalent ranges in particle velocities vary from 0 to 11.5 mm/s. Specifically for simulation 1 where material I was used, all particles were trapped approximately 70 mm above the bottom of the model, occurring this after 40 seconds of simulation. As a result, no particle reached the exit of the model in simulation 1. In addition, the velocity of solids in this simulation is the slowest, that is why only two steps (t = 12 s and t = 40 s) were sufficient to show the results. Recall that material I corresponded to the sands with the largest diameter.

The results for simulation 2 with material II show that after 17 seconds, a first fraction of the particles exits the model through one of the pores, and after 25 seconds, a second fraction of the particles exits through the remaining pores. This differential delay of 8 seconds is possibly favoured by the tortuosity and bifurcations of the pores, which cause the reduction in velocity of the particle motion. This delay in the exit of the particles at some pores is also observed in simulations 3 through 6. At the end of simulation 2 (t = 60 s), it is observed that the particle trapping occurs in the sections of pores that present greater tortuosity in the model.

In simulation 3, which uses material III with particle diameters from 0.3 to 0.6 mm, there are different characteristics to discuss through the steps. For example, the particles reach the maximum velocity of 23.7 mm/s in step 1, while in step 3 (t = 30 s) more particles have accumulated in pores than in simulation 2, where more empty pore spaces are observed. Similarly, in step 4 at the end of the simulation (t = 70 s), fewer trapped particles were observed compared with simulations 1 and 2.

In Scenario 2, shown in Fig. 6, blue colours are again dominant in the pores, but unlike Scenario 1, under these new conditions dark blues predominate as a result of a reduction in simulated seepage velocity. Under this scenario, some particles reach the model outlet for the 3 simulations. This is relevant for PPC performance because the more particles that reach the outlet, the less likely PPC is to clog. Regarding the observations for each of the simulation in this scenario, it can be discussed for instance that the highest value in particle velocities (red zones, 7.28 mm/s), was achieved in some pores of simulation 6 where particles of material III were used in simulations. In simulations 1 and 2, the particles reached the model exit at the same time (t = 240 s), although different materials (I and II) were simulated.

Regarding the time needed to complete steps, it is worth to indicate that in general, simulations in scenario 2 needed more time to complete steps than those of scenario 1. For instance, step 2 was completed in 54 and 61 seconds in scenario 2, while scenario 1 needed 16 and 17 seconds to complete it. Recall that step 2 ended when particles reached the exit of the model in one pore tube.

3.3. Particle trapping in simulated PPC sample

In general, modelling results demonstrate that the percentage of trapped particles in scenario 1 is greater than in scenario 2, as observed in Fig. 7. This implies that a reduced seepage velocity, as that simulated in scenario 2, results in less clogging, contradicting in some way the fact particles reached the exit of the model in all simulations of scenario 2. This dynamic behaviour can be physically explained as follows: a low seepage velocity produces a low drag force, however, gravity force along with the absence of frictional forces permit particles to move longer distances and thus, to reach the exit of the model. Also, a more turbulent flow, such as that simulated with a higher value of seepage velocity, favours the entrapment of particles.

Numerical modelling also reveals the role of grain size in clogging, since the larger the size of the particle the higher the percentage of entrapment, as shown in Fig. 7, where simulations using material I (simulations 1 and 4) presented the higher value of clogging. On the contrary, simulations with material III (simulations 3 and 6), corresponding to the finest particle size, allowed more particles to exit the model. However, when comparing simulations for the same material in both scenarios, e.g. Simulation 1 vs. Simulation 4, it can be observed that a lower seepage velocity of the particles results in a higher percentage of entrapment.

4. Conclusions

Clogging due to the entrapment of solid particles is one of the most recurrent processes affecting the performance of permeable porous concrete (PPC). The implementation of a numerical simulation, using realistic input parameters, can reveal and confirm

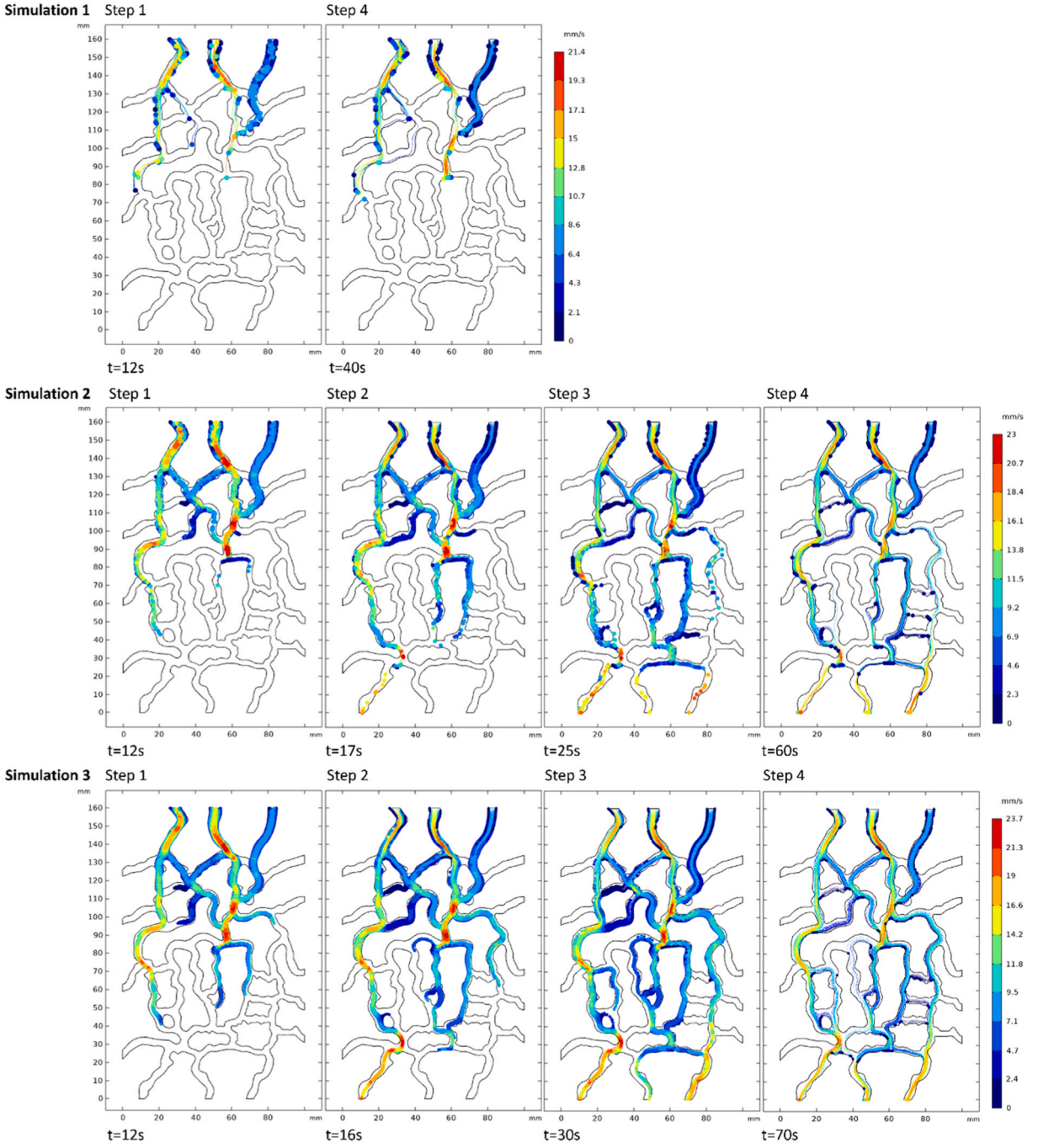

Fig. 5. Position, trajectory, and velocity of solid particles in simulations 1 through 3 for scenario 1. The current time is shown and the seepage velocity used in these simulations is 8.98 mm/s.

insights into the clogging process. This work provides knowledge on processes and parameters such as those related to the hydraulics of the flow of particles through the pores of PPC, the dimensions of the particles favouring clogging, the role of the porous network in the clogging, the time for particles to reach the exit from the PPC sample, among others.

From the experimental work we found that the porosity and permeability varied from 26 % to 28 % and 1.75–1.96 mm/s, respectively, and from these parameters the calculated seepage velocity varied from 8.28 to 9.61 mm/s. From the numerical work, two-dimensional synthetic models with the dimensions of the laboratory samples were simulated in the software COMSOL v.6.2. The parameters obtained in the laboratory were used as inputs in the numerical work, while three types of solid particles, varying in diameter but all in the range of sands, were used as clogging material in two simulated scenarios. The main results of the simulations

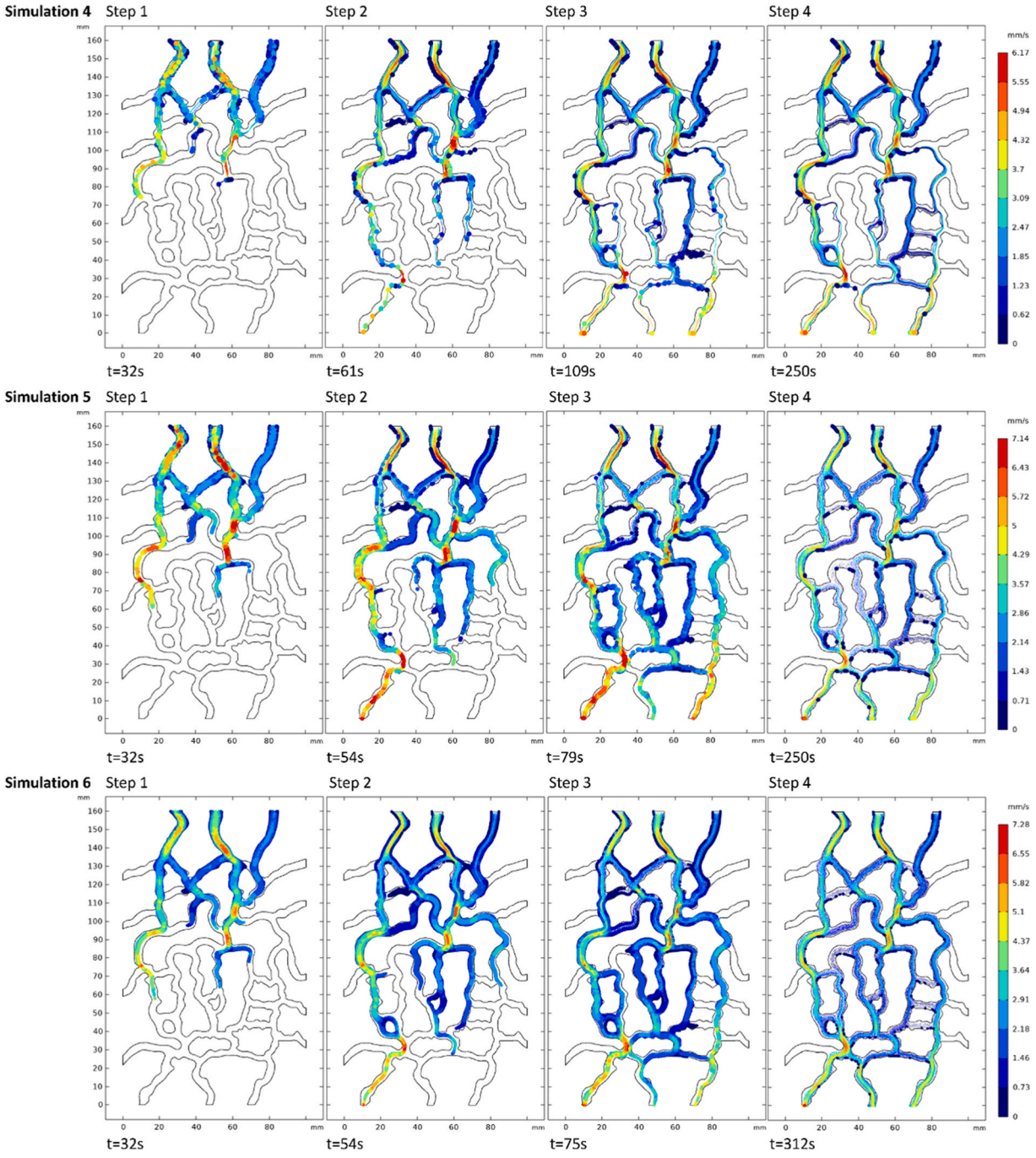

Fig. 6. Position, trajectory, and velocity of solid particles in test simulations 4 through 6 for scenario 2. The current time is shown and the seepage velocity used in this scenario was 2.43 mm/s.

showed that clogging in the PPC is more severe when the diameter of the solid particles ranges from 0.6 to 2.36 mm, and that a reduction of the seepage velocity in the flux of particles entering the PPC results in less clogging. This mentioned particle size corresponds to sand that can be washed away during storms, affecting the PPC in real-world conditions, although it is important to comment that the solids that can be found inside the PPC will depend on the conditions of the application site. Future research should consider validating the numerical model with physical tests of actual hydraulic obstruction behaviour in the PPC to reinforce the reliability of the results.

The findings of the study are applicable to other PPC designs, as long as similar characteristics and properties of permeability, porosity, porous structure and tortuosity are included. However, it is important to note that the PPC mix is very sensitive to variations

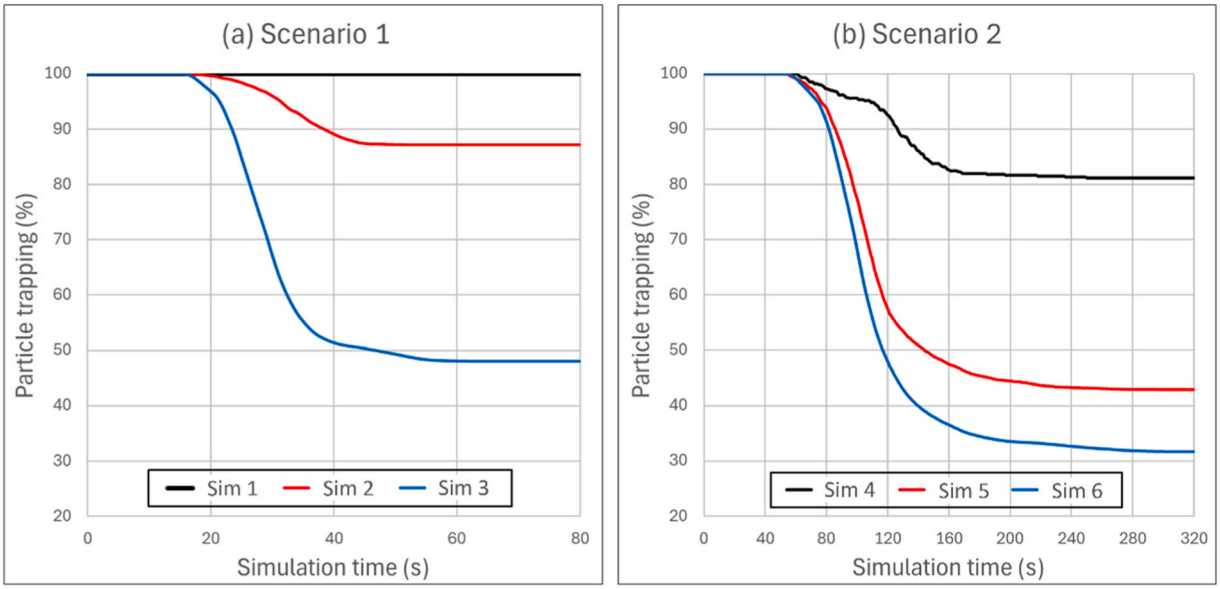

Fig. 7. Variation of the percentage of trapped particles in simulations. Simulations initiate with a 100 % trapping as the particles are released into the model. Once the particles were fully delivered, the percentage began to drop. In fact, the simulation time at which the lines (except for simulation 1) are no longer horizontal corresponds to the time at the end of step 2.

in the grain size curve, so the same properties and characteristics cannot always be obtained. Therefore, further studies are needed to analyze the effect of such curve, as well as the shape and size of the aggregates and their effect on pore tortuosity in real PPC samples. The findings of this study suggest that maintenance strategies should include maintaining good environmental control in areas adjacent to permeable concrete application sites to minimize the ingress of solid particles into the pores.

CRediT authorship contribution statement

Carlos Ignacio Vizcaíno-López: Writing – original draft, Methodology, Conceptualization. **Isaí Gerardo Reyes-Cedeño:** Writing – review & editing. **Anuard Isaac Pacheco-Guerrero:** Writing – review & editing. **Gil Humberto Ochoa-González:** Writing – review & editing. **Lilia Guerrero-Martínez:** Writing – review & editing. **Martín Hernández-Marín:** Writing – review & editing, Software.

Declaration of Competing Interest

The authors declare that they have no known competing financial interests or personal relationships that could have appeared to influence the work reported in this paper

Acknowledgments

Carlos Ignacio Vizcaíno-López is thankful for the financial support from SECIHTI (CONACyT). The authors are also grateful for the outstanding comments of the reviewers, which greatly improved the quality of this manuscript.

Data Availability

Data will be made available on request.

References

[1] M.T. Bashir, A.B. Khan, M.H. Khan, K. Rasheed, S. Saad, F. Farid, Evaluating the implementation of green building materials in the construction sector of developing nations, J. Hum. Earth Future 5-3 (2024), https://doi.org/10.28991/HEF-2024-05-03-015.
[2] R.D. Rosario, A. De La Cruz, M.P. De Guzman, A review of biomineralization as solution for roads and infrastructures concrete sustainability, Civ. Eng. J. 10 (2024) 08, https://doi.org/10.28991/CEJ-2024-010-08-020.
[3] G.J. Khoshnaw, K.H. Younis, W.A. Hamad, A.J. Ismail, G.A.M. Jukil, F.F. Jirjees, H.K. Yaba, S.M. Maruf, Experimental investigation on pervious recycled aggregate concrete made of waste porcelain, -09, Civ. Eng. J. 10 (2024), https://doi.org/10.28991/CEJ-2024-010-09-08.
[4] N. Xie, M. Akin, X. Shi, Permeable concrete pavements: a review of environmental benefits and durability, J. Clean. Prod. 210 (2019) 1605–1621, https://doi.org/10.1016/j.jclepro.2018.11.134.
[5] A. Singh, P.V. Sampath, K.P. Biligiri, Review of sustainable pervious concrete systems: emphasis on clogging, material characterization, and environmental aspects, Constr. Build. Mater. 261 (2020) 120491, https://doi.org/10.1016/j.conbuildmat.2020.120491.

[6] C.H. Aparicio-Uribe, R. Bonilla-Brenes, J. Hack, Potential of retrofitted urban green infrastructure to reduce runoff - a model implementation with site-specific constraints at neighbourhood scale, Urban For. Urban Green. 69 (2022) 127499, https://doi.org/10.1016/j.ufug.2022.127499.
[7] M. Kayhanian, D. Anderson, J.T. Harvey, D. Jones, B. Muhunthan, Permeability measurement and scan imaging to assess clogging of pervious concrete pavements in parking lots, J. Environ. Manag. 95 (2012) 114–123, https://doi.org/10.1016/j.jenvman.2011.09.021.
[8] X. Cui, J. Zhang, D. Huang, W. Tang, L. Wang, F. Hou, Experimental simulation of rapid clogging process of pervious concrete pavement caused by storm water runoff, Int. J. Pavement Eng. 20 (1) (2016) 24–32, https://doi.org/10.1080/10298436.2016.1246889.
[9] A. Kia, H.S. Wong, C.R. Cheeseman, Defining clogging potential for permeable concrete, J. Environ. Manag. 220 (2018) 44–53, https://doi.org/10.1016/j.jenvman.2018.05.016.
[10] G.F.B. Sandoval, I. Galobardes, A. Campos, B.M. Toralles, Assessing the phenomenon of clogging of pervious concrete (Pc): Experimental test and model proposition, J. Build. Eng. 29 (2020) 101203, https://doi.org/10.1016/j.jobe.2020.101203.
[11] R.L.M. Bazarin, F.C. De Lai, C. Naaktgeboren, S.L.M. Junqueira, Boundary effects on the tortuosity and permeability of idealized porous media, Transp. Porous Media 136 (2021) 743–764, https://doi.org/10.1007/s11242-020-01530-w.
[12] J. Cai, J. Chen, J. Shi, Q. Tian, G. Xu, Y. Du, A novel approach to evaluate the clogging resistance of pervious concrete, Case Stud. Constr. Mater. 16 (2022) e00864, https://doi.org/10.1016/j.cscm.2021.e00864.
[13] L.A. Mata, Sedimentation of pervious concrete, Doctoral dissertation, North Carolina State University, Raleigh, 2008.
[14] B. Tong, Clogging effects of Portland cement pervious concrete, MSc Dissertation, Iowa State University, 2011.
[15] B. Eisenberg, K.C. Lindow, D.R. Smith, Permeable pavements, American Society of Civil Engineers, Virginia, 2015.
[16] A.R. Freeze, J.A. Cherry, Groundwater, Prentice Hall Inc, New Jersey, 1979.
[17] P.D. Tennis, M.L. Leming, D.J. Akers, Pervious Concrete Pavements, Portland Cement Association, Illinois, 2004.
[18] J.P. Coughlin, C.D. Campbell, D.C. Mays, Infiltration and clogging by sand and clay in a pervious concrete pavement system, J. Hydrol. Eng. 17 (2012) 68–73, https://doi.org/10.1061/(ASCE)HE.1943-5584.0000424.
[19] N. Hu, J. Zhang, S. Xia, R. Han, Z. Dai, R. She, X. Cui, B. Meng, A field performance evaluation of the periodic maintenance for pervious concrete pavement, J. Clean. Prod. 263 (2020) 121463, https://doi.org/10.1016/j.jclepro.2020.121463.
[20] J. Zhang, M. Guodong, D. Zhaoxia, M. Ruiping, C. Xinzhuang, S. Rui, Numerical study on pore clogging mechanism in pervious pavements, J. Hydrol. 565 (2018) 589–598, https://doi.org/10.1016/j.jhydrol.2018.08.072.
[21] S. Liu, I. Shikhov, C. Arns, Mechanisms of pore-clogging using a high-resolution CFD-DEM colloid transport model, Transp. Porous Media 151 (2024) 831–851, https://doi.org/10.1007/s11242-024-02072-1.
[22] M. Turco, R. Kodešová, G. Brunetti, A. Nilodem, M. Fér, P. Piro, Unsaturated hydraulic behaviour of a permeable pavement: Laboratory investigation and numerical analysis by using the HYDRUS-2D model, J. Hydrol. 554 (2017) 780–791, https://doi.org/10.1016/j.jhydrol.2017.10.005.
[23] X. Nan, Z. Wang, J. Hou, Y. Tong, B. Li, Clogging mechanism of pervious concrete: From experiments to CFD-DEM simulations, Constr. Build. Mater. 270 (2020) 121422, https://doi.org/10.1016/j.conbuildmat.2020.121422.
[24] COMSOL, Particle tracing module user's guide, version 6.2, COMSOL, Burlington, MA, 2022.
[25] American Concrete Institute (ACI), 522R Report on pervious concrete, Farmington Hills, MI, 2010.
[26] American Society for Testing and Materials (ASTM), C192 Standard practice for making and curing concrete test specimens in the laboratory, West Conshohocken, PA, 2000.
[27] American Society for Testing and Materials (ASTM), C127 Standard test method for density, relative density, and absorption of coarse aggregate, West Conshohocken, PA, 2007.
[28] American Society for Testing and Materials (ASTM), C140 Standard test methods for sampling and testing concrete masonry units and related units, West Conshohocken, PA, 2019.
[29] B.M. Das, K., Sobhan, Principles of geotechnical engineering, SI edition, Cengage Learning, Boston, 2014.
[30] V. Andres-Valeri, L. Juli-Gandara, D. Jato-Espino, J. Rodriguez-Hernandez, Characterization of the infiltration capacity of porous concrete pavements with low constant head permeability tests, –4, Water 10 (2018) 480, https://doi.org/10.3390/w10040480.